https://doi.org/10.5194/essd-2026-748
Preprint. Discussion started: 5 November 2026
© Author(s) 2026. CC BY 4.0 License.



Open Access Earth System Science Data Discussions

Analysis-ready European Groundwater Monitoring (EUGM) database

Mariana Gomez[1], Héctor Aguilera[2], Julian Koch[3], Willem Jan Zaadnoordijk[4,7], Georgina Arnó[5], Montse Colomer[5], Benjamin Marchant[6], Bentje Brauns[6], Peter van der Keur[3], Klaus Hinsby[3], and Stefan Broda[1]

[1]Federal Institute for Geosciences and Natural Resources (BGR), Berlin, Germany
[2]Geological and Mining Institute of Spain (IGME-CSIC), Madrid, Spain
[3]Geological Survey of Denmark and Greenland (GEUS), Copenhagen, Denmark
[4]Geological Survey of the Netherlands (TNO-GDN), Utrecht, the Netherlands
[5]Cartographic and Geological Institute of Catalonia (ICGC), Catalunya, Spain
[6]British Geological Survey (BGS), Nottingham, United Kingdom
[7]Water Management Department, Delft University of Technology, Delft, the Netherlands

Correspondence: mariana.gomezospina@bgr.de

Abstract. Reliable pan-European groundwater assessment has long been constrained by fragmented monitoring networks, heterogeneous data formats, and uneven quality-control practices across countries. Within the Geological Service for Europe (GSEU), the groundwater quantity working group addressed this gap by compiling groundwater level (GWL) time series from national and regional geological surveys into the European Groundwater Monitoring (EUGM) database. These GWL time series were harmonized through a standardised workflow that included quality control, resampling to monthly median values, outlier detection, artificial-shift detection, completeness filtering, and gap imputation, resulting in harmonized GWL time series at 15,760 monitoring points. The dataset is complemented by dynamic variables, including precipitation and temperature, and by static variables such as soil properties, lithology, terrain metrics, land cover, population density, and hydrological attributes. In addition, groundwater signatures and Standardised Groundwater Index (SGI) time series were derived from the imputed groundwater records to support the characterization and comparison of groundwater dynamics and anomalies across monitoring points. The dataset is further used to illustrate example applications, including long-term GWL trend analysis and SGI-based cluster classification of temporal GWL dynamics. Together, these data products provide a reproducible basis for groundwater resources assessment, modelling and forecasting across Europe.

1 Background and motivation

Groundwater is fundamental to Europe's water resources, sustaining ecosystem functioning, agricultural productivity, industrial activity, and domestic water supply (EEA, 2024). Its strategic importance has driven extensive monitoring and management efforts at national and transboundary scales (EEA, 2026). In this context, large observational groundwater datasets provide the basis for European-scale analyses, such as the investigation of long-term trends (Chávez García Silva et al., 2024), spatial

https://doi.org/10.5194/essd-2026-748
Preprint. Discussion started: 5 November 2026
© Author(s) 2026. CC BY 4.0 License.



and temporal variability (Baulon et al., 2024), climate-related controls (Baulon et al., 2024), drought impacts (Bloomfield and Marchant, 2013), and anthropogenic influences on aquifer systems (Bloomfield et al., 2019).

In recent years, harmonized large-sample hydrological datasets have become increasingly important in Europe, providing standardised hydrometeorological time series and catchment attributes for regional to continental-scale analyses. Examples include LamaH-CE (Klingler et al., 2021), which offers a self-consistent large-sample surface-water hydrology dataset for Central Europe, and EStreams (do Nascimento et al., 2024), which extends this type of integration to a broader European scale through a harmonized dataset and catalogue of streamflow, hydro-climatic, and landscape information. Comparable efforts have also begun to emerge for groundwater through national and regional compilations as well as broader international initiatives. However, compared with surface-water hydrology, observational groundwater datasets in Europe remain more fragmented, less harmonized, and less readily available for cross-border large-scale analysis.

Existing groundwater data-sharing platforms have improved data availability, but they still fall short of the consistency and harmonization required for regional- to continental-scale numerical and data-driven modelling. The Global Groundwater Information System (GGIS), developed by the International Groundwater Resources Assessment Centre (IGRAC), provides an interactive portal for worldwide groundwater data sharing through the Global Groundwater Monitoring Network (GGMN) (IGRAC, 2026). However, the available records remain heterogeneous in spatial coverage, temporal resolution, and processing level, which limits their direct use for large-scale analysis-ready applications. Similarly, the recently developed GROW dataset (global integrated GROundWater package), built on GGMN, provides a quality-controlled compilation of more than 200,000 time series from 55 countries with daily to yearly temporal resolution, but European coverage remains incomplete (Bäthge et al., 2026). GROW also includes static and dynamic earth system attributes derived mainly from global datasets, which are valuable for broad-scale analyses but do not replace locally specific attributes for site-level interpretation. Another important resource is the European Environment Agency's Waterbase, Water Quantity database (WISE), which contains time series of water-quantity data reported by EEA members and cooperating countries, but differences in reporting frequency among member states and heterogeneous national reporting practices continue to hinder cross-border harmonization (EEA, 2026).

Although high-resolution groundwater level (GWL) records are available through national datasets in Europe, for example in Germany (Ohmer et al., 2026), Switzerland (Collenteur and Moeck, 2026), France (Winckel et al., 2022), and the Netherlands (Zaadnoordijk and Lourens, 2019), as well as through regional institutions (DOV, 2026), pan-European assessments remain constrained by fragmented monitoring networks, uneven data stewardship, and limited access to harmonized observations at continental scale. Together, these limitations reveal a major gap: no existing platform provides a consistently processed pan-European GWL dataset based exclusively on observations with broad spatial and temporal coverage. To address this gap, the groundwater quantity working group of the Geological Service for Europe (GSEU) brings together GWL time series contributed by national and regional geological survey partners into a unified large-scale observational database, providing a common basis for comparative analysis across Europe. This effort also recovers in-situ site attributes, such as well depth, screen length, and aquifer type, wherever they could be retrieved from data providers, adding a more complete set of site attributes than would otherwise be available with readily available continental or global datasets. A key challenge in this process is

https://doi.org/10.5194/essd-2026-748
Preprint. Discussion started: 5 November 2026
© Author(s) 2026. CC BY 4.0 License.



Open Access Earth System Science Data Discussions

that participating partners often served as data coordinators rather than direct data owners, requiring cooperation with the institutions responsible for the original monitoring networks.

The dataset has undergone initial quality control and harmonization and was further preprocessed through gap filtering, outlier and artificial shift detection, and missing-value imputation to produce an analysis-ready product. To support a broad range of hydrogeological applications, we additionally compiled dynamic covariates, static site attributes, SGI, and groundwater signatures for each monitoring location. The resulting dataset provides a unique observational basis for pan-European groundwater analysis. This paper describes the compilation, harmonization, preprocessing, and structure of the dataset, together with its derived variables and intended use in large-scale hydrogeological analysis and modelling.

2 Data gathering and preprocessing

GWL time series were compiled within the GSEU project (Geological Service for Europe, 2026) as part of the groundwater resources workpackage. Participating partners contributed to datasets according to project guidelines developed to ensure a consistent structure and format despite substantial heterogeneities among data providers. These guidelines were designed in line with FAIR principles and defined a common minimum set of requirements, including a minimum record length of five years and a temporal resolution ranging from daily to monthly; annual records were excluded. Partners were also asked to reformat their data into a common template and, where available, to provide additional attributes such as screen length, well depth, aquifer media type, and aquifer type using predefined coding schemes to support dataset harmonization. Submitted datasets were reviewed for completeness and consistency and were subsequently curated and harmonized for integration into the European Geological Data Infrastructure (EGDI) platform (EuroGeoSurveys, 2026). Depending on the data provider, submitted datasets could already reflect prior curation or validation steps, although these were not always documented in a standardised and fully traceable way.

The processing workflow is summarized in Figure 1. Groundwater level records provided by 27 partners underwent quality control to remove stagnant periods (defined as periods with changes smaller than 0.0001 m) longer than one year and physically implausible values (outside range -200 and 2500 m a.s.l) . Time series with daily or weekly resolution were aggregated to monthly median values and reindexed to a strict month-start cadence. Where multiple series existed for a single monitoring point, for example due to different devices or recording resolutions, they were consolidated into a single record. We retained only series with at least five years of data, corresponding to a minimum of 60 monthly observations, a last valid observation after 2000-01-01, and no gap longer than 18 months. The original dataset comprised 34,096 time series, of which 15,760 remained after meeting the final eligibility criteria, covering 24 countries. A conservative automatic outlier detection procedure was then applied to reduce the risk of removing valid measurements of extreme GWL. This implies that some erroneous values may still remain in individual cases. Time series were also screened for persistent artificial level shifts unrelated to genuine hydrological change, for example due to sensor or datum changes; confirmed shifts were reviewed with data providers and corrected or removed where warranted. Missing values were subsequently imputed using a linear mixed model following Marchant et al.

https://doi.org/10.5194/essd-2026-748
Preprint. Discussion started: 5 November 2026
© Author(s) 2026. CC BY 4.0 License.



(2022). Derived products (SGI, groundwater signatures, and trends) were calculated from the imputed time series (Value_comp in Table 5), and clustering was based on SGI time series corresponding to the period 2002-2021 (SGI_2002_2021 in Table 5).

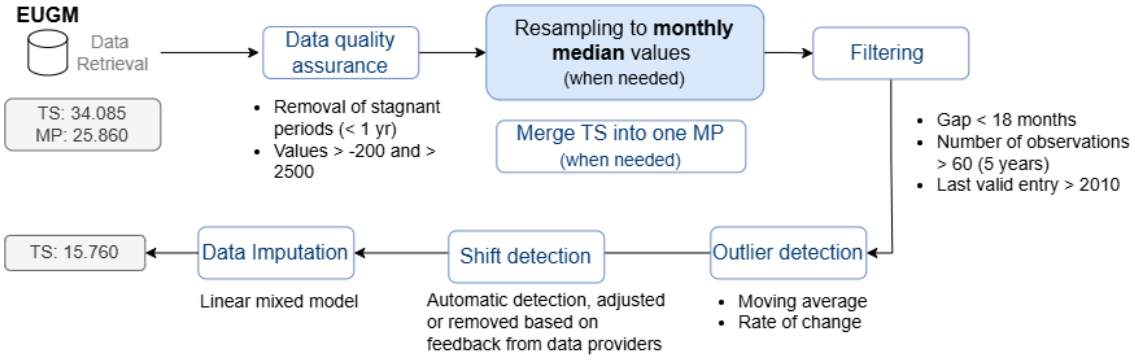


Figure 1. Processing workflow. EUGM: European Groundwater Monitoring Database. TS: time series. MP: monitoring points.

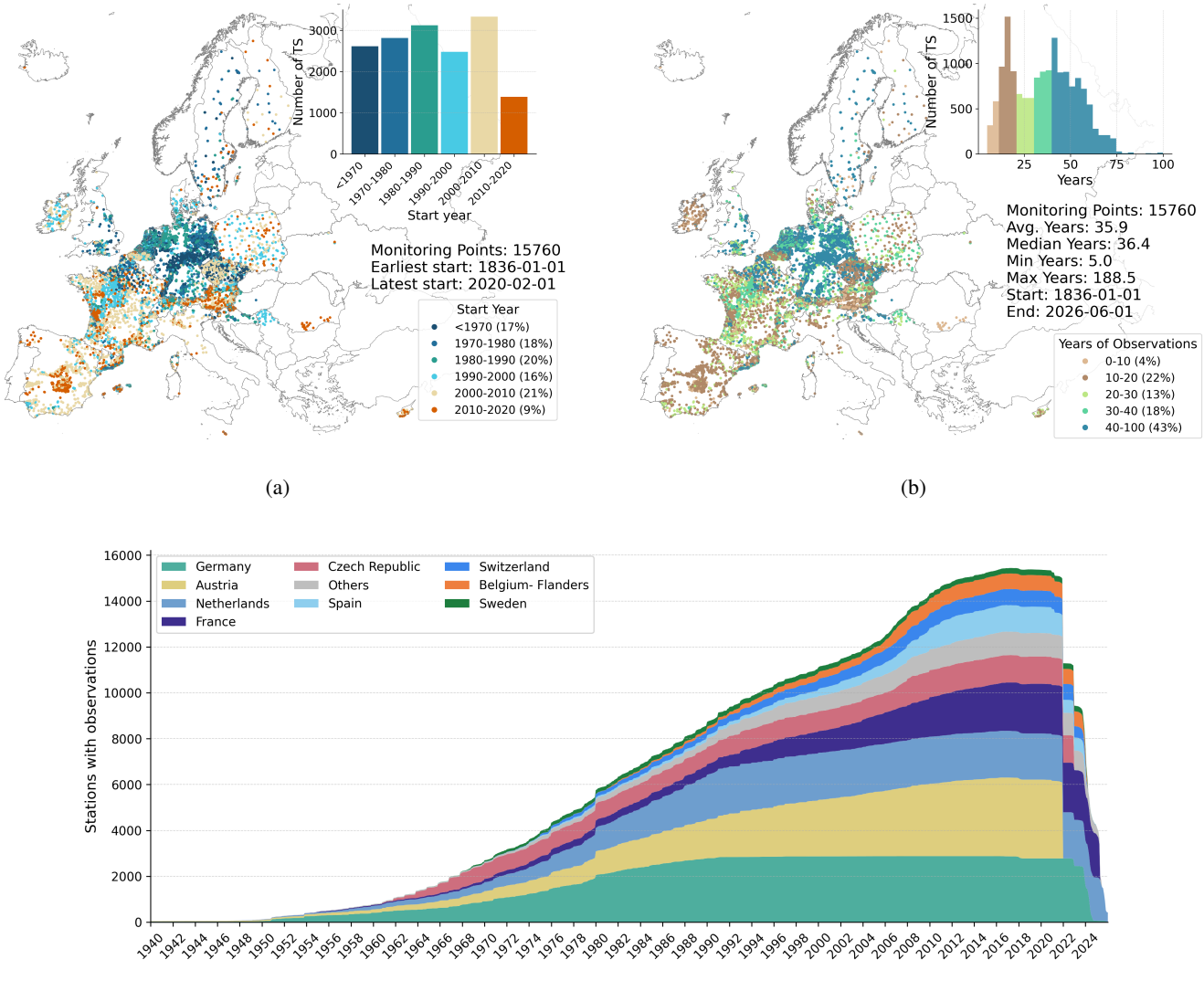
3 European Groundwater monitoring network (EUGM)

3.1 Database characteristics and coverage

After filtering, the EUGM database comprises 15,760 groundwater monitoring points across 24 countries (Fig. 2). To characterize temporal coverage, we mapped the start year of observations and grouped time series by record length (Fig. 2a and 2c). Record length was defined as the time span between the first and last available observation at each monitoring point. The dataset includes many long-term records, i.e., 17 percent of the time series begin before 1970, mainly in Germany, Austria, the Czech Republic, Sweden, the Netherlands and the UK. Later start years are more common in southern European countries such as Spain and Cyprus. Approximately 43% of the time series span between 40 and 100 years. Record lengths range from 5 to 188.5 years, with a mean of 35.9 years and a median of 36.4 years. 17 monitoring points with record lengths exceeding 100 years (located in the UK, Germany) are not shown separately in the figure because they represent only 0.1% of the dataset. In most countries, the number of monitoring points with available observations increases over time and declines in the most recent years (Fig. 2c). This recent decline mainly reflects delays or differences in the delivery of the latest observations by some data providers rather than a reduction in monitoring activity. In some countries, however, reductions in monitoring coverage have occurred due to funding constraints, highlighting the need for continued investment in long-term groundwater monitoring networks. The highest availability of monitoring points with observations occurs between 2010 and 2022. Germany contributes the largest share of observations, followed by Austria, the Netherlands, France, and the Czech Republic.

https://doi.org/10.5194/essd-2026-748
Preprint. Discussion started: 5 November 2026
© Author(s) 2026. CC BY 4.0 License.

Open Access Earth System Science Data Discussions



(a) (b)

(c)

Figure 2. (a) Start year of the GWL time series for each monitoring point. (b) Record length, expressed as categorical classes of the number of years covered by each time series. (c) Number of monthly observations per monitoring point, summarised by country. For visualisation purposes, panel (c) is displayed from 1940 onwards, although 52 time series start before 1940. The countries Cyprus, Denmark, Finland, Croatia, Hungary, Ireland, Iceland, Italy, Malta, Poland, Romania, Serbia, Slovenia, and the United Kingdom are grouped into Others. Administrative boundaries: © EuroGeographics (Eurostat, 2024).

https://doi.org/10.5194/essd-2026-748
Preprint. Discussion started: 5 November 2026
© Author(s) 2026. CC BY 4.0 License.



3.1.1 Groundwater level observations

Table 1 summarizes the monitoring point attributes, including attribute descriptions, units or coding schemes, and data types. Figure 3 shows the spatial distribution of selected attributes, namely AquiferType, AquiferMediaType, depth, and Screen-Length. Monitoring points cover a wide range of hydrogeological settings, as reflected by the AquiferType (Fig. 3a) and AquiferMediaType (Fig. 3b) maps. Aquifer type is available for approximately 55% of the sites and is classified mainly as unconfined, followed by confined aquifers, with smaller subsets of confined subartesian and confined artesian conditions. In confined subartesian aquifers, groundwater rises in a well above the top of the aquifer but remains below the ground surface, whereas in confined artesian aquifers the pressure is sufficient for water to rise above the ground surface. Aquifer media type is available for most monitoring points (98.4%) and is dominated by porous media. The spatial distribution of monitoring points is heterogeneous, with the highest densities in low-elevation areas. Well depth is available for approximately 80% of monitoring points, with a median of 18.4 m and a mean of 44.2 m (Fig. 3c). Screen length is reported for 40.1% of monitoring points, with a median of 2.0 m, a mean of 6.1 m (Fig. 3d).

Out of the 15,760 monitoring points, 856 monitoring points have UTM-coordinates that are identical to another point. Moreover, there are monitoring points located within a few meters of one another. In such situations GWL is measured at multiple depths. Using an arbitrary cut-off distance of 12 meters (see Figure A1), resulted in 13,039 single monitoring points and 1,076 locations with multiple monitoring points. The number of monitoring points for these multi-level locations vary from 2 to 9. Those locations with 2 levels only (n=713) had an average vertical distance between levels of 47.3 meters. The groundwater heads measured at the various depths differ per multi-level location, showing the three-dimensional character of groundwater systems.

4 Quality control of groundwater time series

A contiguous monthly baseline was constructed for each monitoring point by aggregating observations to monthly medians assigned to the month start, with missing months subsequently filled to ensure continuity. Long stagnant periods are set as missing values when consecutive changes persist for more than a year to avoid flatlined artifacts. To reduce edge effects from isolated fragments, any segment of a record separated from the rest of the time series by a gap longer than 18 months is discarded when that gap lies near either end of the observation period: an early fragment is dropped if the separating gap closes before 2010-01-01, and a recent fragment is dropped if the separating gap opens after 2020-01-01. We then filter by completeness and gap length, removing a station only if it has both more than 25% missing values and a maximum gap of at least 3.5 months. Requiring both conditions together, rather than either alone, preserves monitoring points, mainly in Spain, whose sampling frequency was at times coarser than monthly. We require a configurable minimum of valid monthly observations, with a default of 60. Finally, we retain only series whose last valid entry is on or after 2000-01-01 and whose maximum allowed gap length does not exceed 18 months.This threshold was chosen to balance data retention against reliability, and is similar to the value suggested in Marchant et al. (2022).

https://doi.org/10.5194/essd-2026-748
Preprint. Discussion started: 5 November 2026
© Author(s) 2026. CC BY 4.0 License.

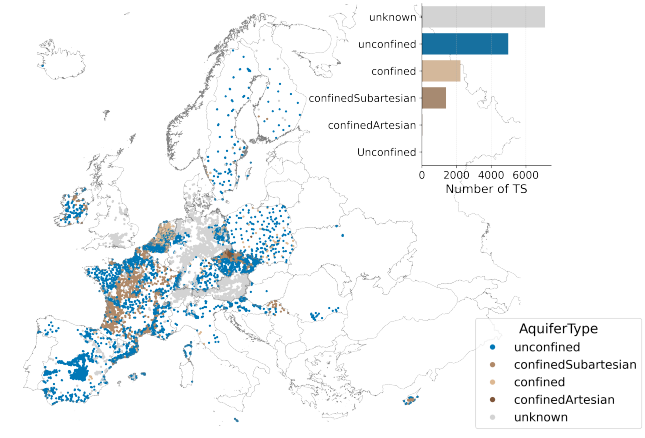


Open Access Earth System Science Data Discussions

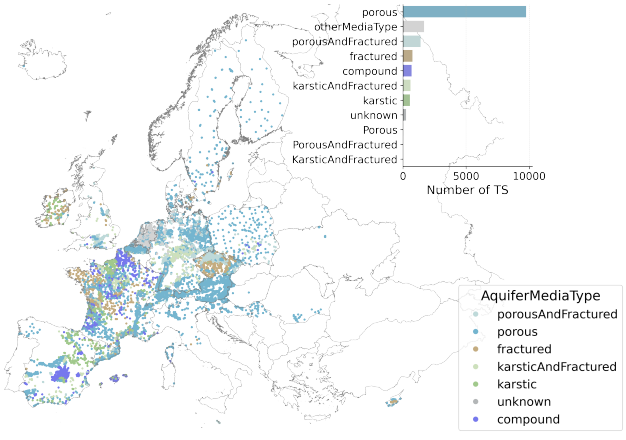
Table 1. Description of groundwater level monitoring point attributes provided by partners.

Attribute	Description	Unit / coding	Data type
id_mp	Unique identification code of the monitoring point, composed of the NUTS level 0 code and the national groundwater monitoring point code.	–	string
region	NUTS level 2 code.	–	string
xutm	X coordinate in metres in the geographic reference system EPSG:3035 ETRS89 / LAEA Europe (https://epsg.io/3035).	m	float
yutm	Y coordinate in metres in the geographic reference system EPSG:3035 ETRS89 / LAEA Europe (https://epsg.io/3035).	m	float
elevation	Altitude in metres above sea level of the land surface where the monitoring point is located, excluding the well head or well curb.	m a.s.l.	float
relatedParty	Organisation related to the monitoring point.	–	string
relatedParty_idMP	Name of the monitoring point in the original source information.	–	string
MPTypeMeasurements	Type of monitoring point measurements.	Quantity / Quality / Both	codelist
MPType	Type of monitoring point.	Non-active well / Pumping well / Well / Piezometer / Water supply	codelist
depth	Vertical depth of the monitoring point measured from the land surface, excluding the well head or well curb.	m	float
ScreenLength	Length of the screen of the well or piezometer.	m	float
RelatedAquifer	Name of the hydrogeological unit or aquifer to which the monitoring point is related.	–	string
AquiferMediaType	Characteristics of the aquifer medium following the INSPIRE codelist AquiferMediaTypeValue.	Porous / Fractured / Karstic / Compound / KarsticAndFractured / PorousAndFractured / Unknown	codelist
AquiferType	Aquifer type following the INSPIRE codelist AquiferType.	Confined subartesian / Confined artesian / Confined / Unconfined / Unknown	codelist

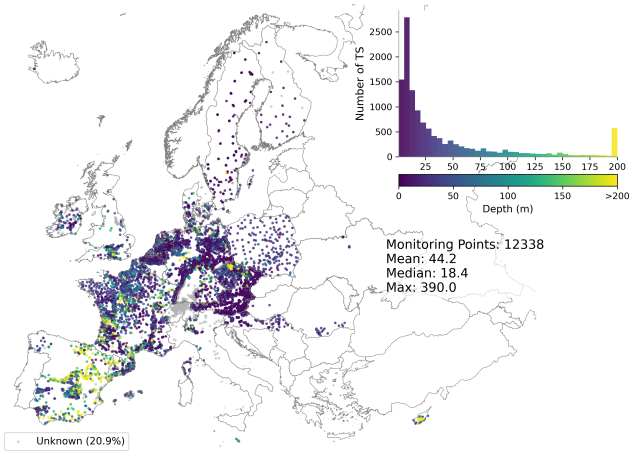
https://doi.org/10.5194/essd-2026-748
Preprint. Discussion started: 5 November 2026
© Author(s) 2026. CC BY 4.0 License.



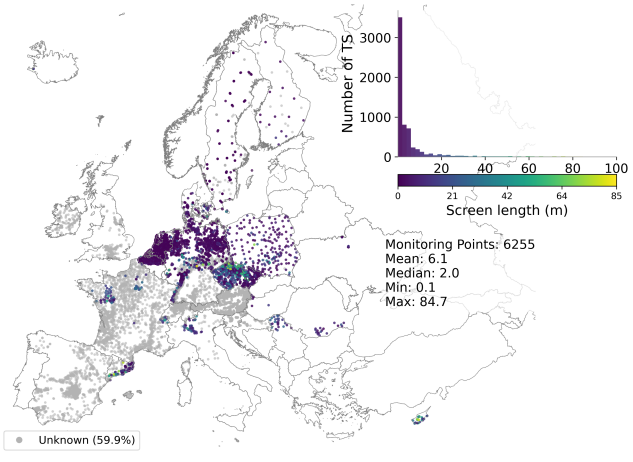
(a)



(b)



(c)



(d)

Figure 3. (a) Aquifer type, (b) Aquifer media type, (c) Well depth, and (d) Screen length shown as maps with corresponding histograms. Values above the 99th percentile were treated as implausible outliers and excluded from the reported statistics and figures for well depth and screen length. Administrative boundaries: © EuroGeographics (Eurostat, 2024).

https://doi.org/10.5194/essd-2026-748
Preprint. Discussion started: 5 November 2026
© Author(s) 2026. CC BY 4.0 License.

Open Access Earth System Science Data Discussions

4.1 Outlier detection

Outliers were identified for each of the monthly baseline time series using two complementary automatic detectors, following practices in ocean water level time series quality control (IOOS, 2016). The first detector used a centered 12-month rolling mean and standard deviation to define a dynamic envelope. Any value with an absolute deviation greater than 3.1 times the rolling standard deviation was flagged, yielding 326 outliers at 242 monitoring points, corresponding to 1.5% of the dataset. The second detector used a rate-of-change test that computed one-step backward and forward absolute differences and compared both to the mean absolute change. A point was flagged only when both adjacent jumps exceeded 10 times the mean change, yielding 206 outliers at 168 stations (1%). A value was treated as an outlier if detected by either detector method resulting in 434 values being detected at 319 stations (2%). The detected values were then converted to NaN to be imputed as described in Sec. 4.3. Because the procedure was applied automatically and only inspected visually for a subset of 100 stations, the thresholds were kept conservative to reduce the risk of removing genuine observations during seasonal high- or low-water periods. As a result, some erroneous values may still remain in individual time series.

4.2 Shift detection

GWL time series can contain persistent level shifts unrelated to genuine hydrological change, for example due to a change in measurement reference, sensor, or reporting practice. These were identified using a standalone rolling-median approach: for each station, every month was tested as a candidate breakpoint by comparing the median of the preceding window to the median of the following 12-month window. This raw step was then compared to how much the water level typically fluctuates from month to month at that station, so a jump only counted as a likely shift if it was clearly larger than the station's normal month-to-month variation. Persistence checks were applied so that only shifts remaining separated for several months were retained. Only the single strongest candidate shift was evaluated per station; a station with more than one genuine shift would only have its most prominent one flagged.

This procedure flagged 201 monitoring points across the dataset as showing a likely artificial shift. These were reviewed with the relevant data providers where feasible. Overall, 9 stations were corrected using provider-supplied replacement series and 36 stations were removed from the dataset following this review. The remaining 156 flagged stations are retained in the dataset unchanged and are marked with the boolean shift detection column, so that users can identify and, if needed, exclude measuring points affected by shifts or further investigate these series for their specific application. Users should particularly consider this flag when analysing derived quantities that may be sensitive to persistent level shifts, such as long-term trends and groundwater signatures.

4.3 Data Imputation

We used a linear mixed model and the Best Linear Unbiased Predictor (BLUP) for data imputation following Marchant et al. (2022). The model splits variability into fixed and random effects. The fixed effects are linear relationships with a series of covariates which capture a linear temporal trend, a long-term component via a decadal spline, a seasonal component consisting

https://doi.org/10.5194/essd-2026-748
Preprint. Discussion started: 5 November 2026
© Author(s) 2026. CC BY 4.0 License.



of a sinusoid with a period of 12 months, and meteorological memory through a weighted average of the previous 60 months of rainfall and temperature where the weights are determined from estimated impulse response functions. The random effects are the residuals of this linear model and include temporal correlation. In an extension of the Marchant et al. (2022) methodology, a Box-Cox transform was applied to the data to relax the assumption that the residuals follow a Gaussian distribution.

For each monitoring point, the parameters of the model (namely the linear regression coefficients, parameters of the temporal correlation function and parameters of the impulse response function) were estimated by maximum likelihood. The fitted model was then used within the BLUP to predict the expected GWL and the variance of this prediction for each month where observations were not available. For imputation dates prior to 1955, the model was refitted without the rainfall and temperature terms. Data imputation was validated on artificial gaps introduced in a subset of 600 GWL time series. The typical gap patterns were first identified following Bikše et al. (2023) and applied to 500 monitoring points, random gap patterns were introduced in the remaining 100. When these time series were standardised to mean zero and unit variance, the Nash–Sutcliffe model efficiency coefficient (NSE) across the artificial gaps was 0.83.

The workflow described in Marchant et al. (2022) estimates five variants of the model for each monitoring point to decide which of the covariates should be included in the final model. This was impractical for the number of monitoring points considered in this study and therefore all covariates were included for all monitoring points. This could inhibit the interpretability of the models if the impacts of different covariates confound each other. However, in the validation tests it only led to a small decrease in accuracy. Imputation uncertainty is reported as half of the width of the 68th prediction interval of the imputed values where the observed values have been scaled to have unit variance. If this value is zero, then the imputed value is exact. If the distribution of groundwater levels were Gaussian and the imputation values were predicted simply by the mean of the observed groundwater levels then the uncertainty value would be 1. Amongst the EUGM data, around 1 in 400 of the imputed values have an uncertainty value greater than 1. These generally occur for boreholes where the observed values are skewed and on dates where high groundwater levels are expected. They reflect the uncertainty associated with predicting groundwater levels which might be larger than any of the observed values.

5 Dynamic and static attributes

5.1 Dynamic features

We compiled time series of groundwater-relevant meteorological variables sourced from ERA5 (Hersbach et al., 2020) via the Copernicus Climate Data Store at all monitoring points in the EUGM database. The processed data originate from the ERA5-Land reanalysis dataset at monthly resolution with a spatial resolution of 0.1 degree covering a period from 1950 to 2025. The selected variables are stated in Table 2 and also include processed variables, such as relative humidity, calculated from air temperature and dewpoint temperature, and the Standardised Precipitation Index (SPI) with different aggregation periods for which a rolling sum of the precipitation has been calculated (Kumar et al., 2009). Coastal measuring points may be placed outside the ERA5-Land grid and for those the nearest ERA5-Land cell has been utilized. Figure 4 displays an example of dynamic features for a single station over the period 2000-2025.

https://doi.org/10.5194/essd-2026-748
Preprint. Discussion started: 5 November 2026
© Author(s) 2026. CC BY 4.0 License.



Open Access Earth System Science Data Discussions

Table 2. Dynamic meteorological variables used in this study. Variables t2m, sp, rh, and tp were extracted from ERA5-Land at 0.1° monthly resolution. SPI variables were derived from total precipitation.

Variable	Explanation	Unit
t2m	2 m air temperature	K
sp	Surface pressure	Pa
rh	Relative humidity	%
tp	Total precipitation	m/day
spi1	Standardised Precipitation Index with 1-month aggregation period	unitless
spi6	Standardised Precipitation Index with 6-month aggregation period	unitless
spi12	Standardised Precipitation Index with 12-month aggregation period	unitless
spi48	Standardised Precipitation Index with 48-month aggregation period	unitless



Figure 4. Example of dynamic meteorological features extracted from ERA5-Land for a single monitoring point (id AT_300012).

https://doi.org/10.5194/essd-2026-748
Preprint. Discussion started: 5 November 2026
© Author(s) 2026. CC BY 4.0 License.



Open Access Earth System Science Data Discussions

5.2 Static site features

For each measuring point various static features have been processed to distinguish groundwater-relevant variability driven by landscape characteristics. The features comprise the natural system, such as topography, soil and hydrogeology, as well as the anthropogenic system, such as land cover and population density. The native resolution of the features varied, and some originated from gridded datasets while others were vector shapefiles. The anthropogenic features are quasi-static and represent multiyear variability. Table 3 summarizes the static variables used in this study; Figure 5 illustrates four representative examples (clay and sand content of the soil, nearest river Strahler order, and lithological classification at aggregation level 5) and their spatial distribution.

Table 3. Static environmental variables as a complement to attributes described in Table 1.

Type	Variable	Explanation	Unit	Resolution	Source
Soil	clay	Mean clay content, 0–200 cm	g/kg	1 km	SoilGrids (Poggio et al., 2021)
	sand	Mean sand content, 0–200 cm	g/kg		
	silt	Mean silt content, 0–200 cm	g/kg		
	cfvo	Mean coarse fragment content, 0–200 cm	g/kg		
	soc	Mean soil organic carbon, 0–200 cm	dg/kg		
	bdod	Mean bulk density, 0–200 cm	cg/m^3		
Terrain	dem	Elevation	m	1 arcsec	EU-DEM (DHI GRAS, 2014)
	slope	Slope	degrees		
Hydrology	nearest_river_distance	Distance to nearest river	m	62 km^2 catchments, polyline	Ecrins (EEA, 2012)
	nearest_river_strahler	Strahler order of nearest river	unitless		
	distance_strahler_eq_1	Distance to nearest first-order river	m		
	DSD_1–3	Multiorder Hydrologic Position for Europe, Divide-to-Stream Distance (DSD), orders 1–3	m	1 arcsec	EUMOHP (Nölscher et al., 2022)
	LP_1–3	Multiorder Hydrologic Position for Europe, Lateral Position (LP), orders 1–3	m		
	SD_1–3	Multiorder Hydrologic Position for Europe, Stream Distance (SD), orders 1–3	m		
Hydrogeology	ihme_level1–5	Lithological classification of the aquifers at five aggregation levels	classification	1:1,500,000	IHME1500_v12 (BGR, 2019)
	ihme_aquif_name	Aquifer productivity and rock type	classification		
	ihme_saltintrus	Saltwater intrusion	binary		
Geology	igme_age	Pre-Quaternary geology age	classification	1:5,000,000	IGME5000 (BGR, 2016)
	igme_structure	Geological structure within 1 km	classification		
Population	pop_sum_yyyy	Population within 10 km radius	population	30 arcsec	GHS-POP (Pesaresi et al., 2024)
Land use	corine_level1_yyyy	Land cover, level 1	classification	100 m	CORINE (CLMS and EEA, 2020)

https://doi.org/10.5194/essd-2026-748
Preprint. Discussion started: 5 November 2026
© Author(s) 2026. CC BY 4.0 License.

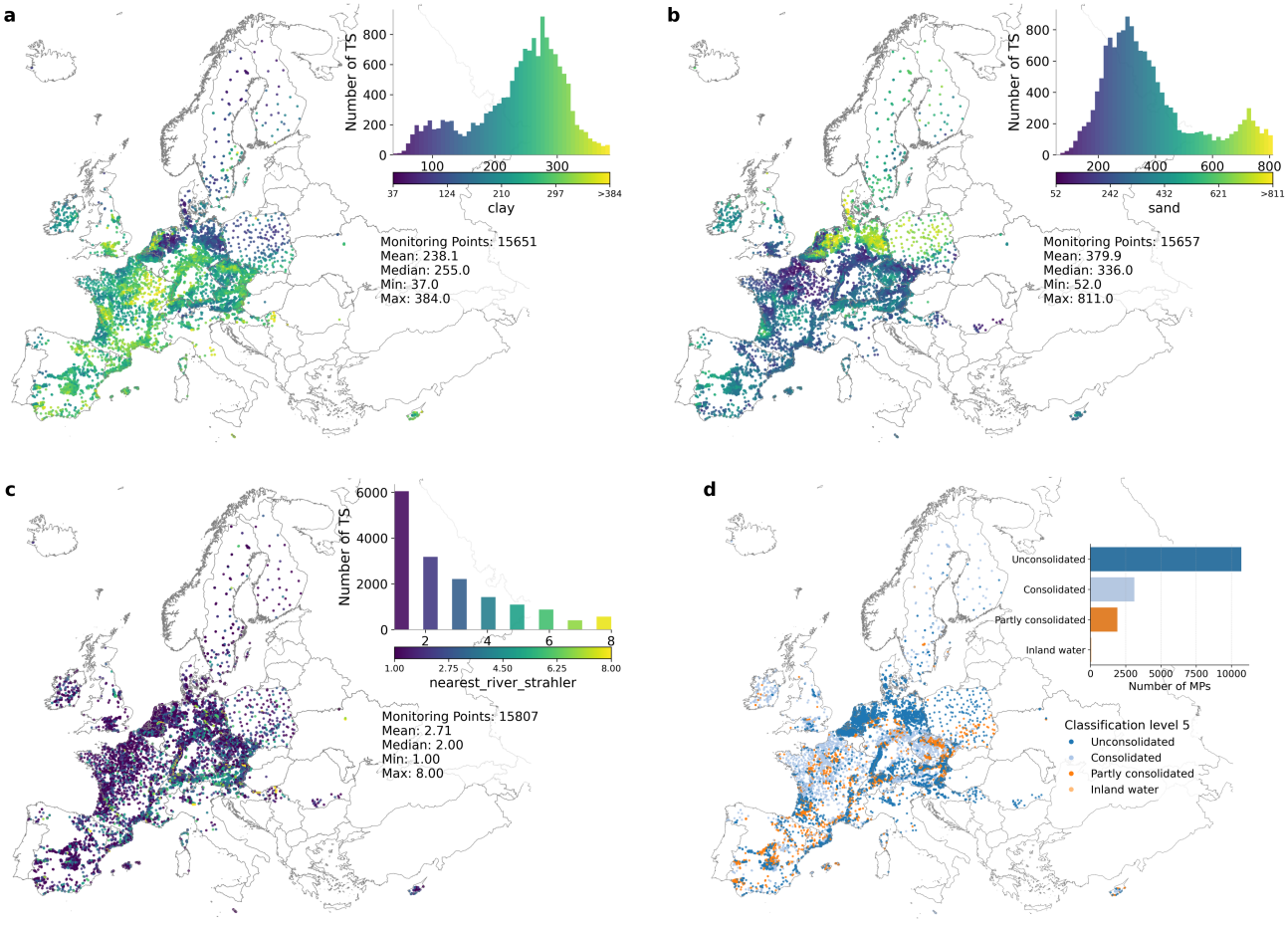


Figure 5. Static features at the ground surface of the monitoring points: a clay content, b sand content, c nearest river Strahler order, and d classification level 5. Insets show the corresponding feature distributions. Administrative boundaries: © EuroGeographics (Eurostat, 2024).

5.3 Groundwater time series derived attributes

5.3.1 Standardised groundwater index (SGI)

Standardised Groundwater Index (SGI) time series were computed from the harmonised monthly GWL time series for each monitoring point using the method of Bloomfield and Marchant (2013) over the full available period of the series. For each station, monthly GWL were transformed to a standardised anomaly index by estimating the empirical cumulative probability of observations for each calendar month and mapping these probabilities to the standard normal distribution. This procedure removes differences in magnitude and seasonality among stations and enables comparison of groundwater conditions across aquifer systems. SGI values close to zero indicate normal GWL for the specific month, negative values indicate below-normal

https://doi.org/10.5194/essd-2026-748
Preprint. Discussion started: 5 November 2026
© Author(s) 2026. CC BY 4.0 License.



GWL, and positive values indicate above-normal GWL. In addition to the SGI computed over each station's full period of record, one further version was computed using a fixed reference period, 2002–2021, following the same procedure. The reference period was selected based on spatial and temporal data coverage. Using a common period across all stations, rather than each station's own record length, improves comparability of the index between monitoring points and enables direct comparison with derived products defined over the same window, such as the 2002–2021 trend analysis in Sect. 6.

5.3.2 Groundwater signatures

Groundwater signatures were estimated over the full available period of record for each monitoring point, using the signature functions implemented in Pastas v1.14.0 (Collenteur et al., 2019), following the definitions listed in Table 4. We selected signatures suitable for monthly time series and adapted those whose original formulation assumes a finer temporal resolution, namely *date_min*, *date_max*, *cv_date_min*, *cv_date_max*, *colwell_constancy*, and *colwell_contingency*. In addition, *magnitude* was defined alternatively to obtain a broader distribution of values, and *autocorr_time* was computed independently following the same definition, due to a version-dependent inconsistency identified in Pastas's autocorrelation function for regularly-spaced monthly time series. Figure 6 summarizes the resulting values for six signatures across monitoring points and illustrates their distributions. Regarding the groundwater signatures shown in Figure 6, the *cv_date_max*, which summarizes the variability of annual maxima, has a median of 0.75 and a mean of 1.31, suggesting that most sites have relatively consistent peak timing while a subset shows much greater variability. *autocorr_time*, describing system memory, has a median of 2.0 and a mean of 2.18, indicating typically short persistence with only a limited tail toward longer memory. Seasonal structure, represented by *colwell_contingency*, is generally weak to moderate, with a median of 0.10 and a mean of 0.12. In contrast, *interannual_variation* is much more skewed, with a median of 1.32 but a substantially higher mean of 2.92, implying that although many wells show modest year-to-year variability, some experience pronounced multi-annual fluctuations. The annual peak level metric, *mean_annual_maximum*, is comparatively stable, with a median of 0.66 and a mean of 0.65. Finally, *magnitude*, which reflects the overall range of variation, also shows strong skewness, with a median of 1.33 and a mean of 2.86, indicating that most wells have moderate ranges while a smaller number exhibit much larger amplitudes.

6 Example applications: trends and Clustering

In the following, two example applications are presented to demonstrate the potential of the EUGM database for investigating groundwater dynamics at European scale. In the first application, trends have been calculated for the time series that contain values for all months in the period 2002-2021. The trends have been calculated using the non-parametric Mann-Kendall-Sen approach as implemented in the Dutch Groundwater head viewer (TNO-GDN, 2024). A variant of the Mann-Kendall test has been used to determine whether the times series has a significant increasing or decreasing trend. Depending on the outcome of the Kruskal-Wallis test, seasonal variation is accounted for and if necessary, a resampling to quarterly values is applied to eliminate autocorrelation. The trend slope is calculated as the Theil-Sen slope or seasonal Sen's slope.

https://doi.org/10.5194/essd-2026-748
Preprint. Discussion started: 5 November 2026
© Author(s) 2026. CC BY 4.0 License.

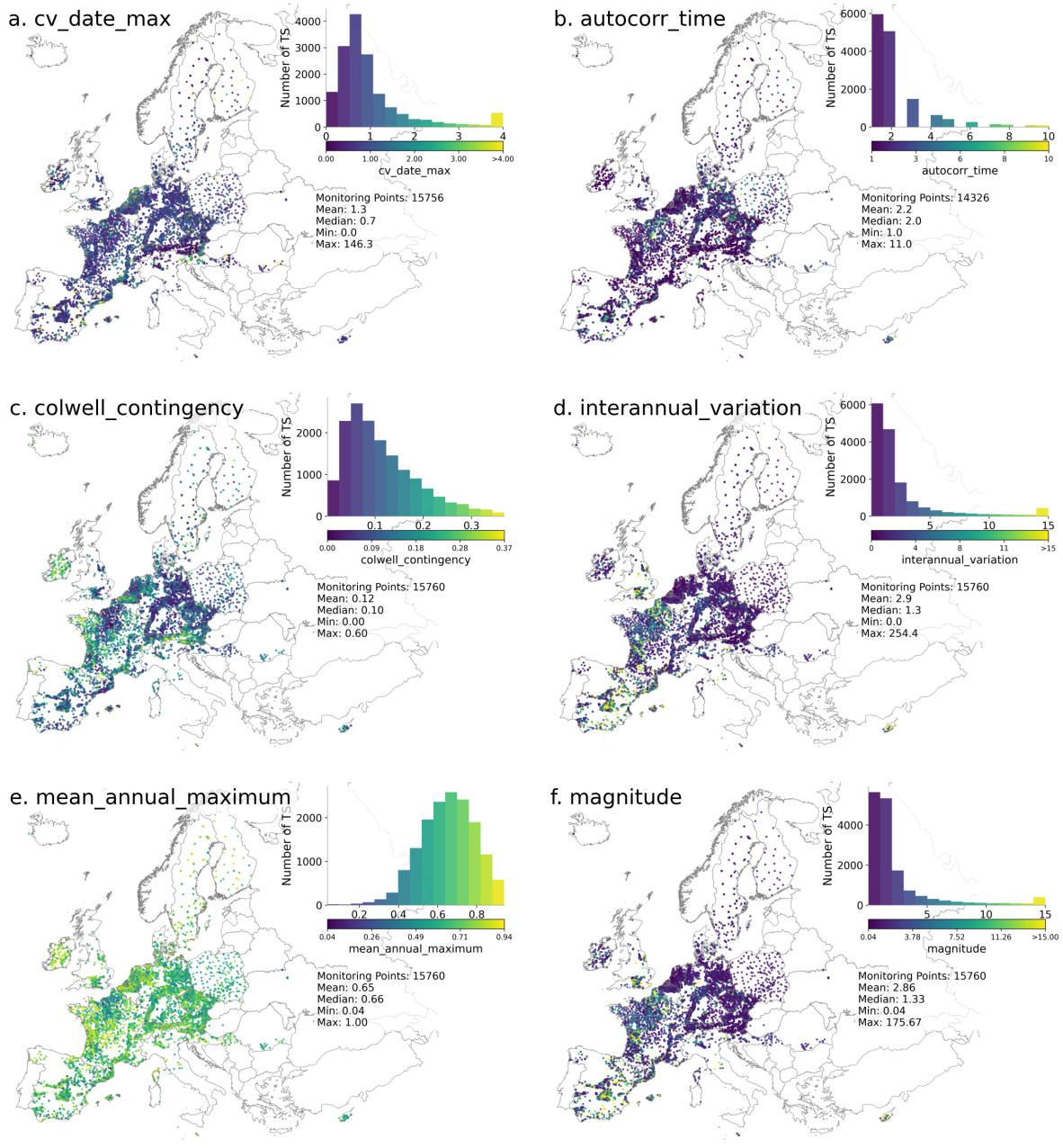


Figure 6. Map of six groundwater signatures. Each panel shows point-wise values with a histogram, summarizing timing (*cv_date_max*), memory (*autocorr_time*), seasonal structure (*colwell_contingency*), interannual variability (*interannual_variation*), annual peak level (*mean_annual_maximum*), and range (*magnitude*). Values above the 99th percentile were capped for visualization purposes only, to prevent a small number of extreme values from dominating the colour scale; reported summary statistics are computed on the uncapped data. Administrative boundaries: © EuroGeographics (Eurostat, 2024).

https://doi.org/10.5194/essd-2026-748
Preprint. Discussion started: 5 November 2026
© Author(s) 2026. CC BY 4.0 License.



Open Access Earth System Science Data Discussions

Table 4. Groundwater signatures computed using Pastas v1.14.0 (Collenteur et al., 2019). The signatures *date_min*, *date_max*, *cv_date_min*, *cv_date_max*, *colwell_constancy*, and *colwell_contingency* were adapted for monthly groundwater time series, *magnitude* is reported using an alternative definition, and *autocorr_time* was recomputed independently following the same definition, to ensure correct behaviour at monthly resolution.

Name	Description	Units / range
date_min	Mean timing of the annual minimum on a circular month-of-year scale, accounting for the December to January wrap-around.	Month of year (1–12, fractional)
date_max	Mean timing of the annual maximum on a circular month-of-year scale, accounting for the December to January wrap-around.	Month of year (1–12, fractional)
cv_date_min	Variability of annual minimum timing on a circular month-of-year scale. Higher values indicate more variable timing.	Dimensionless (≥ 0)
cv_date_max	Variability of annual maximum timing on a circular month-of-year scale. Higher values indicate more variable timing.	Dimensionless (≥ 0)
autocorr_time	Smallest lag at which the autocorrelation function drops below a cutoff of 0.8.	Integer monthly steps (≥ 1), or NaN
colwell_constancy	Entropy-based measure of overall stability, quantifying how consistently the series remains within a narrow range of values over time, independent of season.	0–1 (higher = more constant)
colwell_contingency	Entropy-based measure of seasonal structure, quantifying how strongly values depend on the time of year.	0–1 (higher = more seasonally structured)
cv_period_mean	Relative variability of the typical monthly level, computed as the coefficient of variation of the monthly mean values.	Dimensionless (≥ 0)
parde_seasonality	Measure of seasonal contrast based on monthly means relative to the overall mean, defined as the difference between the maximum and minimum monthly Pardé coefficients.	Dimensionless (≥ 0)
avg_seasonal_fluctuation	Mean annual difference between the average of the 3 highest monthly heads and the average of the 3 lowest monthly heads within each year.	m
interannual_variation	Mean of the ranges across years in the average of the 3 highest monthly heads and the average of the 3 lowest monthly heads.	m
bimodality_coefficient	Heuristic modality measure derived from skewness and kurtosis: $(\mathrm{skewness}^2 + 1)/\mathrm{kurtosis}$.	Dimensionless
mean_annual_maximum	Mean of the annual maximum head.	m
duration_curve_slope	Slope of the head-duration curve between lower and upper percentiles.	m per unit exceedance
duration_curve_ratio	Ratio of the head-duration curve between the 10th and 90th percentiles, defined as $Q(0.1)/Q(0.9)$.	Dimensionless (> 0; higher = flatter head duration curve)
magnitude	Range of the time series, defined here as the 95th percentile minus the 5th percentile.	m

Figure 7 shows the monitoring points with a significant trend; for the multi-point locations identified in Section 3 and Appendix A1, where several piezometers monitor different depths at the same location, only the uppermost piezometer is shown. In order to show the distribution of moderate trends, all points with an absolute value greater than 20 cm per year have been put into single bins that contain a large number of points (89 with a declining and 109 with an increasing trend greater than 20 cm/yr) but cover a limited area.

There are more locations with significant declining than increasing trends, but at the European scale there are few regions with exclusively either declining or increasing trends. This spatial heterogeneity illustrates the importance of local and regional controls on groundwater level trends and highlights the need for caution when interpreting aggregated patterns at the European scale.

https://doi.org/10.5194/essd-2026-748
Preprint. Discussion started: 5 November 2026
© Author(s) 2026. CC BY 4.0 License.

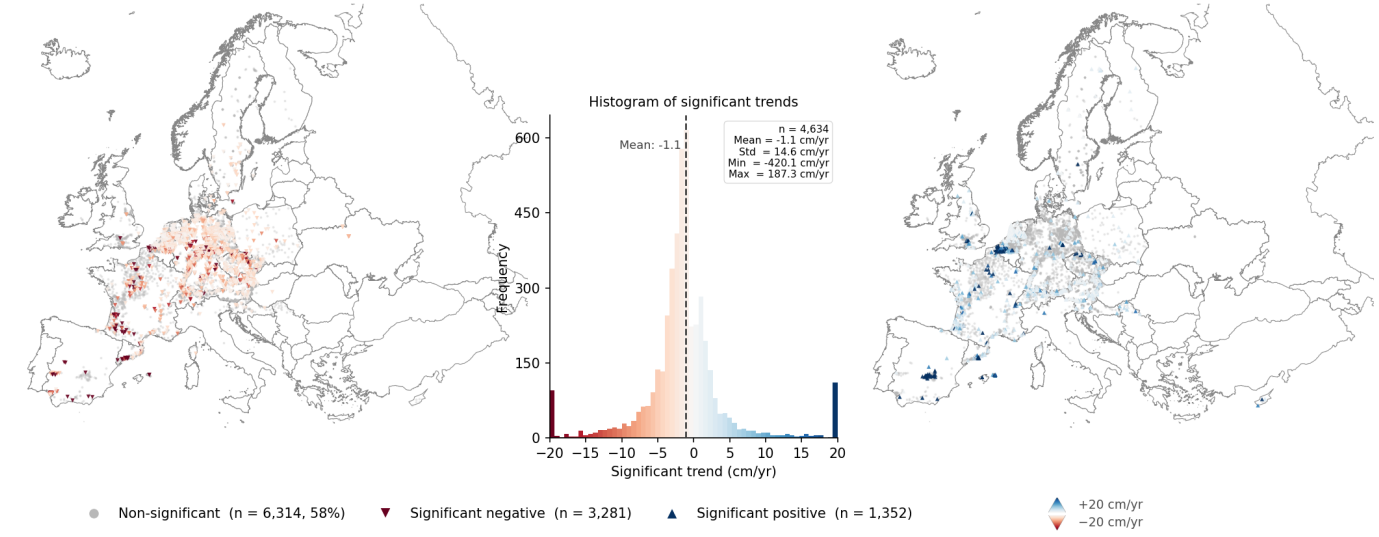


Figure 7. Monitoring locations showing a significant declining trend (red, left) or increasing trend (blue, right) for the period 2002-2021. Administrative boundaries: © EuroGeographics (Eurostat, 2024).

In the second application, SGI for the period 2002-2021 were used to explore common temporal dynamics across monitoring points through cluster analysis (Fig. 8). Clustering was performed using k-means applied to the SGI time series (Bloomfield et al., 2015), for a range of cluster numbers (n = 2–15). Initially, an elbow plot was used to identify the appropriate number of clusters located at the inflection point of the within-cluster variance. However no distinct inflection point was apparent, the reduction in within-cluster variance diminished progressively across this range, indicating that solutions within it capture the main structure of the data while avoiding unnecessary complexity.

Inspection of the clustering results across this range shows that increasing the number of clusters from five to seven progressively resolves meaningful spatial and temporal differences, including the separation of large regional groupings. At lower cluster ($n < 7$) numbers, groundwater levels from the Anglo–Paris Basin, a large sedimentary basin that extends across southern England, the English Channel, and northern France, were not resolved as a distinct group, but were instead grouped within a cluster characterised by a weakly increasing trend. This reflects the comparatively damped and delayed response of chalk aquifers, resulting in smooth SGI time series that mask shorter-term variability and reduce their separability from other sites at coarser clustering resolutions, i.e., lower number of clusters.

At eight clusters, further differentiation becomes evident, particularly separating monitoring points in south-west Germany, Switzerland, Austria and the Netherlands from those in south-east Germany and the Czech region. These clusters display distinct SGI behaviour, with differences in both the temporal variability and the timing of high and low SGI periods (Fig. A2). This additional split reflects hydrologically meaningful variation rather than over-fragmentation.

Increasing the number of clusters beyond eight, primarily results in subdivision of an existing group with very similar SGI characteristics and geographical distributions, without providing additional interpretative value. We therefore selected eight

https://doi.org/10.5194/essd-2026-748
Preprint. Discussion started: 5 November 2026
© Author(s) 2026. CC BY 4.0 License.

clusters as a balance between capturing key hydrogeological differences and maintaining a parsimonious and interpretable solution

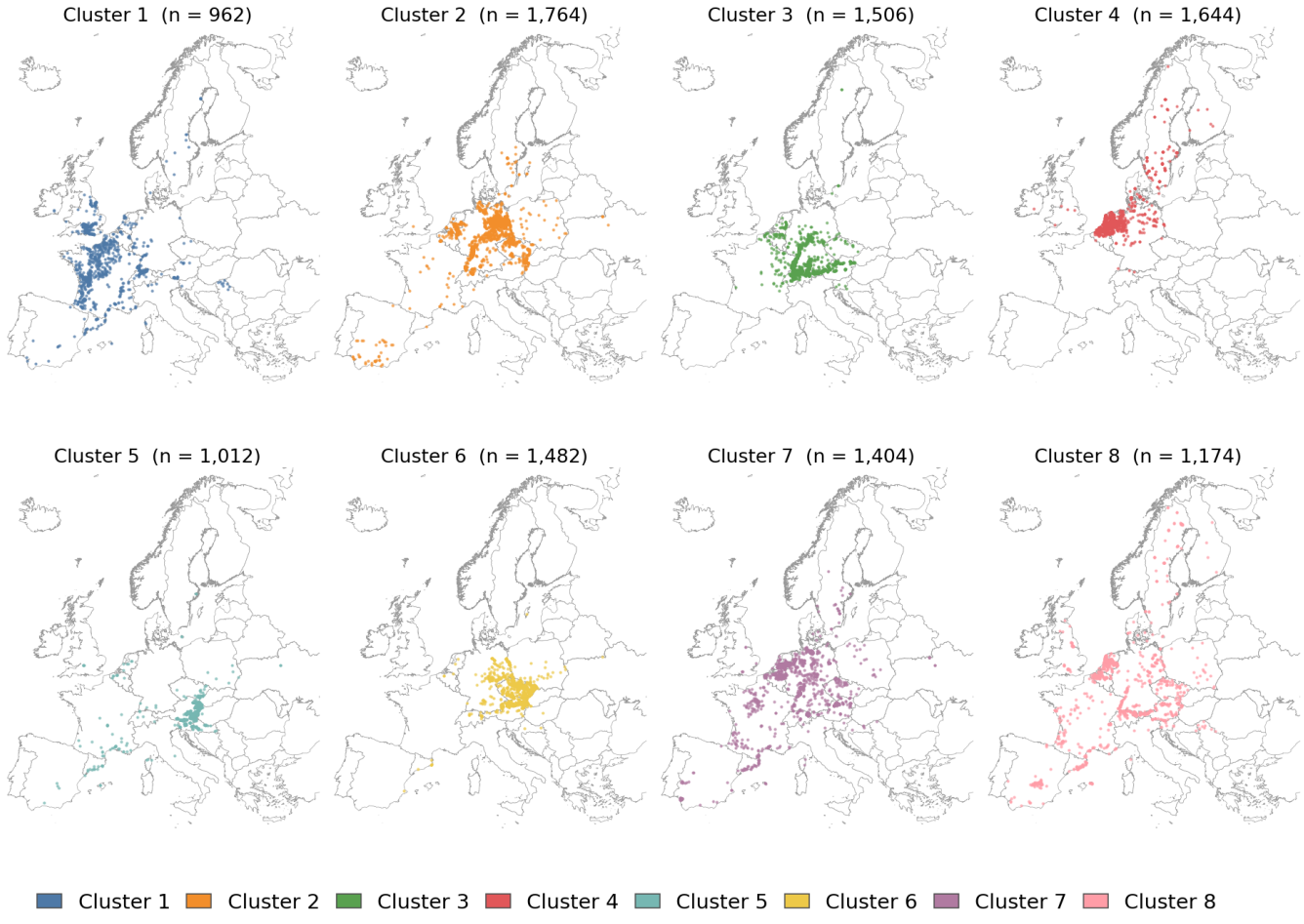


Figure 8. Spatial distribution of the eight groundwater dynamics clusters identified from k-means clustering of the standardised groundwater level (SGI) time series over the period 2002-2021 (Section 6). Each panel shows the monitoring points assigned to one cluster, plotted over the same European extent; the number of monitoring points per cluster (n) is given in each panel title. Administrative boundaries: © EuroGeographics (Eurostat, 2024).

7 Database structure

The database is organised into separate tables for monitoring point attributes, GWL time series, time-series derived GWL indices, dynamic and static site variables, and derived GWL signatures, trends, and clusters. Each table uses the monitoring

https://doi.org/10.5194/essd-2026-748
Preprint. Discussion started: 5 November 2026
© Author(s) 2026. CC BY 4.0 License.



point identifier (id_mp) as its key, allowing the different data components to be linked and updated independently as new observations, attributes, or derived products become available. Table 5 summarises the main files, their attributes, and their internal structure, forming a modular and extensible foundation designed to accommodate additional observations and derived products as the EUGM dataset evolves.

The attributes of EUGM_gwl.csv reflect the successive stages of processing applied to each record, from the initial quality control through to the complete series used in the downstream analyses. Value_org as the monthly value after the quality control steps described in Sect. 2 (stagnant period and implausible value removal), prior to outlier detection. Value then carries this same series with the outliers identified in Sect. 4.1 additionally removed and converted into NaN. Imputed_value contains the imputed values described in Sect. 4.3, covering both genuine gaps and the points removed as outliers. Uncert_imp is the imputation uncertainty described in Sect. 4.3, reported only where Imputed_value is populated. Value_comp combines Value with Imputed_value to provide a complete, gap-free series, and is the series used to compute groundwater signatures (Sect. 5.3.2), SGI and SGI_2002_2021 (Sect. 5.3.1.) and the trend and cluster analyses (Sect. 6). shift_detected flags whether the station was identified by the shift-detection algorithm (Sect. 4.2) as showing a likely artificial level shift.

Table 5. Overview of the main output files and their attributes. In every file, id_mp is used as the row index (unique per monitoring point). For the two time series files, EUGM_gwl.csv and dynamic.csv, TimeInstant additionally identifies each row together with id_mp; all other files have exactly one row per monitoring point. In all cases, the columns listed under Attributes are the variable names. Missing or not-applicable values are stored as empty fields (NaN) throughout, except AquiferType and AquiferMediaType, which use the categorical value "Unknown" for the same purpose.

Attributes	Filename
region, xutm, yutm, elevation, relatedParty, relatedParty_idMP, MPTypeMeasurements, MPType, depth, ScreenLength, RelatedAquifer, AquiferMediaType, AquiferType	./EUGM_mp.csv
Value_org, Value, Imputed_value, Uncert_imp, Value_comp, SGI, SGI_2002_2021, shift_detected	./EUGM_gwl.csv
t2m, sp, rh, tp, spi1, spi6, spi12, spi48	./dynamic.csv
clay, sand, silt, cfvo, soc, bdod, dem, slope, nearest_river_distance, nearest_river_strahler, distance_strahler_eq_1, dsd1–3, lp1–3, sd1–3, ihme_level1–5, ihme_aquif_name, ihme_saltintrus, igme_age, igme_structure, pop_sum_yyyy, corine_level1_yyyy, corine_level3_yyyy	./static.csv
date_min, date_max, cv_date_min, cv_date_max, autocorr_time, colwell_constancy, colwell_contingency, cv_period_mean, parde_seasonality, avg_seasonal_fluctuation, interannual_variation, bimodality_coefficient, mean_annual_maximum, duration_curve_slope, duration_curve_ratio, magnitude	./gw_signatures.csv
tac_testP_mon_RP, tac_testTau_mon_RP, tac_slope_mon_RP, tac_slope_sig_mon_RP, tac_slope_intercept_mon_RP, tac_slopeCI_low_mon_RP, tac_slopeCI_up_mon_RP, cluster_number	./trends_cluster.csv

https://doi.org/10.5194/essd-2026-748
Preprint. Discussion started: 5 November 2026
© Author(s) 2026. CC BY 4.0 License.



Open Access Earth System Science Data Discussions

8 Uncertainties and limitations

The EUGM database combines records from 27 partners across 24 countries, and the monitoring networks, measurement practices and quality-control procedures applied before data delivery differ substantially among data owners. Based on information from the data-providing partners during data compilation, these procedures range from formalised multi-level systems combining automated plausibility checks; expert review and final verification within a certified quality-management framework, or monthly verification cycles with case-by-case review of outliers together with field operators; to periodic visual inspection by hydrogeologists and annual manual review and adjustment. In several countries, quality control is delegated to regional or basin authorities whose procedures differ among regions, for example the federal states in Germany, the regional environmental agencies in Italy, the river basin authorities in Spain, and the national environmental regulators of England, Wales and Scotland in the United Kingdom. For some partners, the quality control applied at the data-owner stage is not documented. Logger drift and reference errors are typically corrected against manual dip measurements where these are available. The level of validation also differs within individual records: historical data generally undergo more intensive expert validation than recent data, which in some networks are not checked for errors or outliers before release. Consequently, the most recent part of a time series is likely to be less thoroughly validated than earlier periods.

Further differences in data quality arise from processing and station selection before delivery. Some providers aggregated high-frequency data before submission using different statistics; for instance, hourly data in France were aggregated to daily maxima to represent the level least affected by pumping drawdown, while in the Netherlands, the value closest to 12 Noon was selected for each day with multiple measurements. The monthly medians in EUGM are therefore derived from inputs that were not aggregated in the same way across countries. Station selection criteria also vary: in Denmark, abstraction wells and wells close to large abstractions were excluded, whereas most other networks include monitoring points that may be affected by human activity. The degree of anthropogenic influence and the hydrogeological settings represented therefore vary between countries in ways that cannot be fully characterised from the available metadata.

Within EUGM, the preprocessing pipeline was deliberately conservative. Because the same automated procedure had to be applied across a large and heterogeneous monitoring network, thresholds were selected to perform robustly across the full dataset rather than being optimised for any single provider. This design favours retaining genuine hydrological signal, including legitimate extreme values, over flagging every possible anomaly, since discarding real information at continental scale would be the greater cost. As a result, erroneous measurements linked to local influences or provider-specific artefacts may remain in individual time series, and users with site-specific knowledge of a particular station or region are encouraged to apply additional checks. Temporal coverage, while substantial (mean 35.9 years), peaks between 2010 and 2022, with declining recent observations reflecting delivery lags rather than monitoring cessation. Imputed values carry an uncertainty (Uncert_imp, Sect. 4.3) that users should account for, for example in sensitivity analyses. In addition, attribute completeness varies, with approximately 21% of monitoring points lacking depth information, reflecting legacy data collection practices.

The dynamic and static variables are derived from external datasets and inherit their uncertainties, as well as the mismatch between gridded or mapped values and point observations. The meteorological variables originate from ERA5-Land, a land

https://doi.org/10.5194/essd-2026-748
Preprint. Discussion started: 5 November 2026
© Author(s) 2026. CC BY 4.0 License.


reanalysis rather than direct observations. Although provided at 0.1° resolution, it is driven by coarser ERA5 atmospheric forcing, and only temperature, humidity and pressure are adjusted for elevation, whereas precipitation is interpolated without downscaling (Muñoz-Sabater et al., 2021). Values therefore represent grid-cell conditions rather than conditions at the monitoring point; differences are expected to be largest in complex terrain and for coastal points, for which the nearest valid land cell was used. The SPI inherits the uncertainty of the precipitation input and depends on the fitted distribution and calibration period; as it was computed over each station's record, which in some cases is shorter than the 30 years recommended by the WMO, values are not strictly comparable between stations with different record periods. The static variables were sampled at the location of each monitoring point from datasets with native resolutions ranging from 1 arcsec to map scales of 1:5,000,000. For the hydrogeological and geological maps (IHME1500 at 1:1,500,000 and IGME5000 at 1:5,000,000), the mapping scale implies a positional generalisation of the order of kilometres, and the classes describe the mapped surface or regional aquifer rather than the screened interval of the monitoring point. Soil properties from SoilGrids are model predictions with their own spatially variable uncertainty (Poggio et al., 2021), CORINE land cover has a minimum mapping unit of 25 ha, and population data from GHS-POP are modelled estimates obtained by disaggregating census counts, with the values for 2025 and 2030 representing projections. These variables should therefore be interpreted as descriptors of the regional setting of a monitoring point rather than as site-specific measurements.

9 Data reuse notes

For most applications, we recommend to use the attribute Value where only observed data are required, while Value_comp is intended for applications requiring gap-free series. Model performance should preferably be evaluated on observed values only, since imputed values are model predictions that partly depend on meteorological covariates and are smoother than observations, which may inflate performance metrics. Monitoring points flagged with shift_detected should be checked or excluded, particularly for trend analyses and groundwater signatures, and Uncert_imp can be used to exclude uncertain imputed values. Because co-located multi-level monitoring points and the uneven network density mean that monitoring points are not independent samples, spatially grouped validation is advisable for data-driven models and continental-scale analysis. Comparisons between regions are best based on standardised indices (SGI, SGI_2002_2021) rather than absolute levels, and apparent trends should be interpreted in the light of local hydrogeological knowledge. The spatial density of the monitoring network is uneven across Europe, with some countries contributing substantially more monitoring points than others. Southern European countries are generally underrepresented in the dataset, reflecting lower monitoring densities and data availability compared to northern and western Europe. Consequently, continental-scale results should not be interpreted as a spatially representative assessment of European groundwater conditions. Finally, the monthly medians used throughout this dataset may not adequately capture the short-term dynamics of fast-responding aquifer systems, such as karst or shallow unconfined aquifers, where groundwater levels can fluctuate substantially within days to weeks (Bakalowicz, 2005); slower-responding systems (e.g., confined or low-permeability aquifers) are comparatively less affected by this temporal aggregation.

https://doi.org/10.5194/essd-2026-748
Preprint. Discussion started: 5 November 2026
© Author(s) 2026. CC BY 4.0 License.

Open Access Earth System Science Data Discussions

10 Concluding remarks

Groundwater is a valuable resource for Europe, and to better understand and manage this resource coordinated efforts across countries are needed to harmonize monitoring data and build large-scale datasets. Such datasets are essential for identifying broad spatial and temporal patterns, supporting cross-border analyses, and enabling the development of comparable methods at the European scale. Meaningful analyses and practical decision-support solutions further require datasets that are consistent, standardised, and easily accessible. The current EUGM dataset contains 15,760 monitoring points with observational records ranging from 6 years to more than 100 years, together with their associated attributes. To further enrich the database, we extracted static and dynamic features and computed the SGI and groundwater signatures. As example applications, we derived long-term trend statistics and an SGI-based cluster classification of groundwater dynamics across the dataset, which supports hydrogeological analysis at the European scale. Beyond the trend and cluster results presented here, the EUGM can support drought propagation studies, for which the scarcity of consistent, large-scale groundwater observations has been identified as a key limitation (Hellwig et al., 2020). It is also intended to support model calibration across transboundary aquifer systems (Naz et al., 2023), and lower the technical barrier for applying both numerical groundwater models and machine-learning frameworks across the continent. At the same time, users should be aware of the heterogeneity inherited from differing national monitoring and quality-control practices, the uncertainty of imputed values, and the regional rather than site-specific character of the environmental variables, and follow the given recommendations.

Future development priorities include near-real-time data integration for a subset of stations, expansion of quality-flagged raw data availability for uncertainty quantification, and incorporation of additional dynamic components such as snowmelt influences and groundwater abstraction records. Selected monitoring points are expected to be updated through the EGDI platform (EuroGeoSurveys, 2026), creating a pathway for continued data integration and operational use. We hope that future initiatives will build on this foundation and further expand the dataset at the European scale. The compilation of this resource was only possible through the close collaboration of the project partners.

https://doi.org/10.5194/essd-2026-748
Preprint. Discussion started: 5 November 2026
© Author(s) 2026. CC BY 4.0 License.



Open Access Earth System Science Data Discussions

Code and data availability. The processed EUGM dataset described in this paper is available at Zenodo https://doi.org/10.5281/zenodo.21891416 (Gomez et al., 2026b), released under a CC BY 4.0 license. The preprocessing, plotting, and trend-analysis code can be found in the GitHub repository (Gomez et al., 2026a).

Appendix A: Supplementary Figures

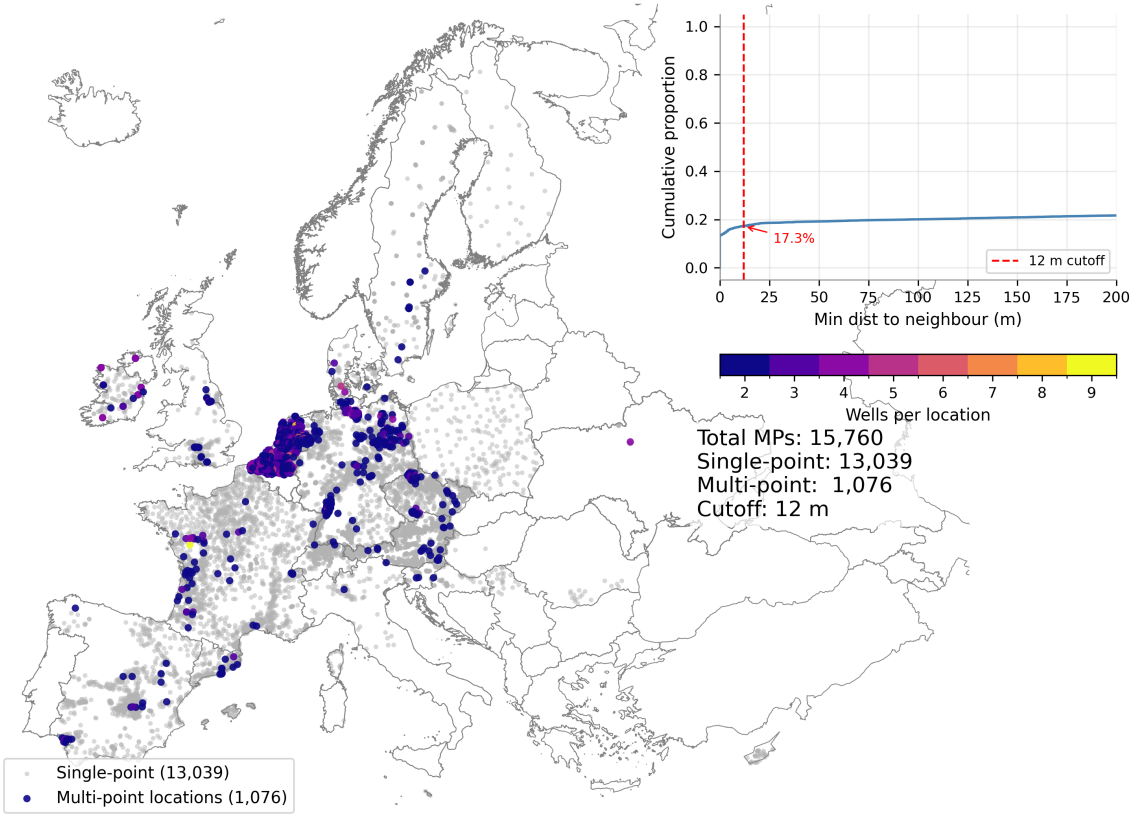


Figure A1. Spatial distribution of single- and multi-point monitoring locations across the EUGM dataset (n = 15,760). Grey markers denote stations whose nearest neighbour exceeds 12 m (n = 13,039). Coloured markers denote groups of two or more co-located wells within a 12 m horizontal radius (n = 1,076 groups, 2,721 total monitoring points), with colour encoding the number of wells per group (2–9). The inset shows the cumulative distribution function of the minimum horizontal distance to the nearest neighbour. The distribution rises sharply to 17.3 % within 12 m, then flattens to a near-plateau. Administrative boundaries: © EuroGeographics (Eurostat, 2024).

https://doi.org/10.5194/essd-2026-748
Preprint. Discussion started: 5 November 2026
© Author(s) 2026. CC BY 4.0 License.

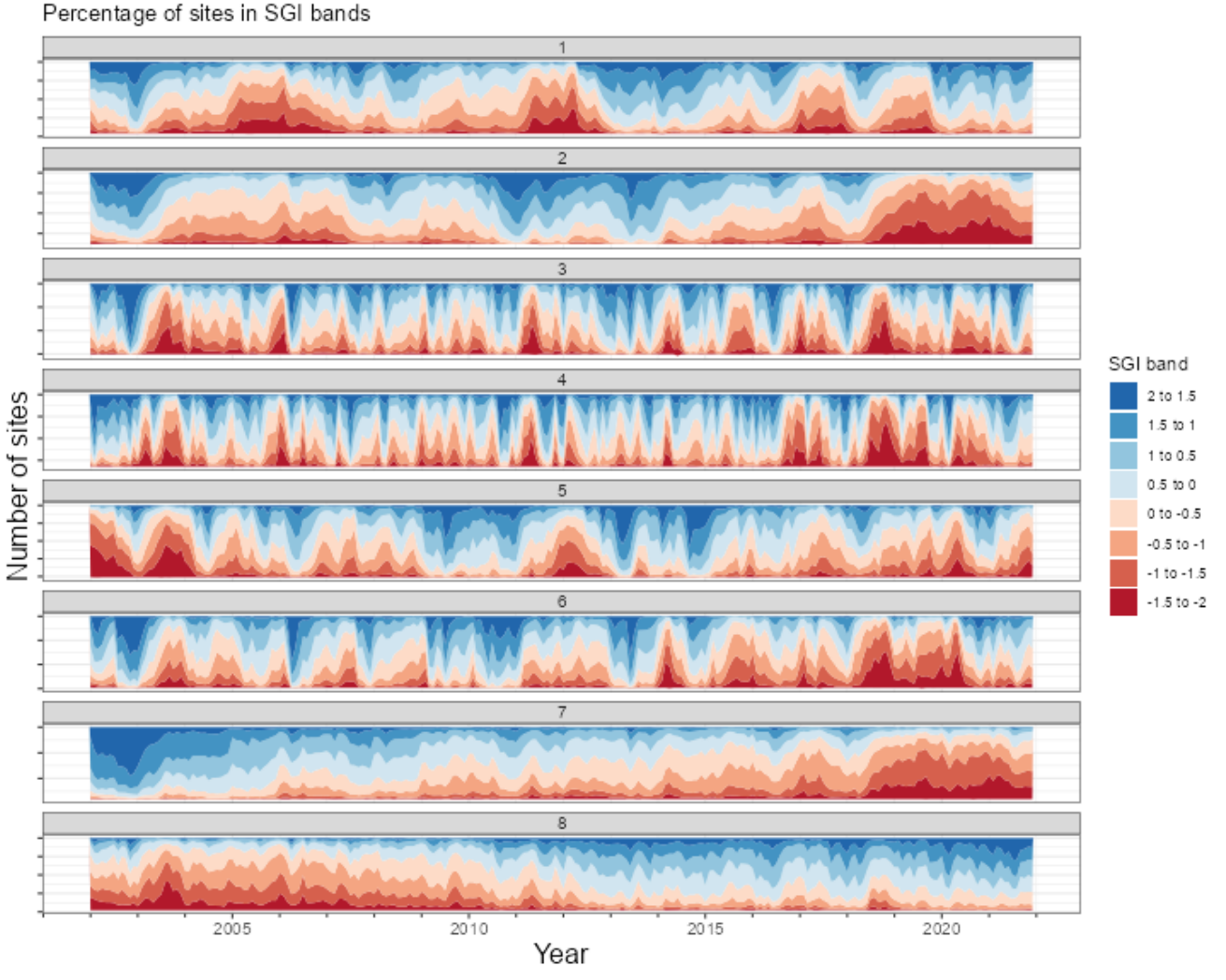


Figure A2. Percentage of monitoring points within each cluster (Section 6) falling into each Standardised Groundwater Index (SGI) band, following the drought/wetness classification of Bloomfield and Marchant (2013). Negative SGI values indicate below-normal (dry) groundwater conditions and positive values indicate above-normal (wet) conditions within the analysis period 2002-2021.

https://doi.org/10.5194/essd-2026-748
Preprint. Discussion started: 5 November 2026
© Author(s) 2026. CC BY 4.0 License.



Author contributions. MG designed the data-processing workflow, database structure, and harmonization and quality-control procedures, with contributions from HA, JK, and BM. MG also carried out the groundwater signature analysis, performed the analyses used to describe and validate the dataset, prepared the visualizations, and wrote the original draft of the manuscript. HA, JK, and WJZ extracted the static and dynamic features and contributed to the data-processing workflow, the analyses used to describe and validate the dataset, and the visualizations. BM contributed to the data-processing workflow, data imputation, and SGI calculation. GA and MC contributed to the conception and design of the dataset, data provision, and harmonization and quality control. BB, SB, PvdK, WJZ, and KH contributed to writing, review, and editing. All authors reviewed the manuscript and approved the final version.

Competing interests. The contact author has declared that none of the authors has any competing interests.

Acknowledgements. This work was done with funding from the European Union via the GSEU-programme (Geological Service for Europe, 2026). We gratefully acknowledge the data contributions provided by the many regional and national geological surveys and partner institutions: the Geologische Dienst Nederland (TNO-GDN, the Netherlands), Bureau de Recherches Géologiques et Minières (BRGM, France), Hrvatski Geološki Institut (HGI-CGS, Croatia), Państwowy Instytut Geologiczny – Państwowy Instytut Badawczy (PGI-NRI, Poland), Institut Cartogràfic i Geològic de Catalunya (ICGC, Spain), Česká geologická služba (CGS, Czechia), the Department of Environment, Climate and Communications – Geological Survey Ireland (GSI, Ireland), Agencia Estatal Consejo Superior de Investigaciones Científicas – Instituto Geológico y Minero de España (CSIC-IGME, Spain), Bundesanstalt für Geowissenschaften und Rohstoffe (BGR, Germany) and the German federal states, Geološki zavod Slovenije (GeoZS, Slovenia), Istituto Superiore per la Protezione e la Ricerca Ambientale (ISPRA, Italy), the Institute of Geological Sciences of the National Academy of Sciences of Ukraine (IGS, Ukraine), the Geological Survey of Serbia (GZS, Serbia), the Ministry of Agriculture, Rural Development and Environment of Cyprus (GSD, Cyprus), Sveriges geologiska undersökning (SGU, Sweden), the Geological Survey of Denmark and Greenland (GEUS, Denmark), Szabályozott Tevékenységek Felügyeleti Hatósága (SZTFH, Hungary), GeoSphere Austria (GeoSphere, Austria), Eesti Geoloogiateenistus (EGT, Estonia), Íslenskar Orkurannsóknir (ISOR, Iceland), Vlaamse Milieumaatschappij (VMM, Belgium - Flanders), Elliniki Archi Geologikon kai Metalleftikon Erevnon (H.S.G.M.E., Greece), Geologian Tutkimuskeskus (GTK, Finland), the energy and water agency, Malta(EWA, Malta), Institutul Geologic al României (IGR, Romania) and the British Geological Survey (BGS, UK). Data for Switzerland were obtained from the Swiss Groundwater Database (Collenteur and Moeck, 2026). Note: Data owners might differ with data providers, please refer to Table 1 for details regarding each monitoring point. B. Brauns, and B. Marchant publish with the permission of the Director of the British Geological Survey (UKRI).

Claude (Anthropic) was used to assist with language editing of the manuscript and with structuring and organizing the data-processing code.

https://doi.org/10.5194/essd-2026-748
Preprint. Discussion started: 5 November 2026
© Author(s) 2026. CC BY 4.0 License.



References

Bakalowicz, M.: Karst groundwater: a challenge for new resources, Hydrogeology Journal, 13, 148–160, https://doi.org/10.1007/s10040-004-0402-9, 2005.

Bäthge, A., Vargas, C. R., Lischeid, G., Collenteur, R., Cuthbert, M., Fleckenstein, J., Flörke, M., de Graaf, I., Gnann, S., Hartmann, A., Huggins, X., Moosdorf, N., Wada, Y., Wagener, T., and Reinecke, R.: A Global-Scale Time Series Dataset for Groundwater Studies within the Earth System, Scientific Data, 13, 401, https://doi.org/10.1038/s41597-026-06966-1, 2026.

Baulon, L., Fossa, M., Massei, N., Flipo, N., Gallois, N., Fournier, M., Dieppois, B., Danaila, L., Allier, D., and Bessiere, H.: Sensitivity of groundwater levels to low-frequency climate variability in a large watershed, Science of The Total Environment, 957, 177 636, https://doi.org/10.1016/j.scitotenv.2024.177636, 2024.

BGR: The 1:5 Million International Geological Map of Europe and Adjacent Areas (IGME5000-EU, INSPIRE-compliant dataset), https://inspire-geoportal.ec.europa.eu/srv/api/records/7fdad3e8-67c1-43cf-ad9f-aa025c58ecd3, iNSPIRE-compliant dataset following the Geology Data Specification D2.8.II.4_v3.0, 2016.

BGR: International Hydrogeological Map of Europe, https://doi.org/10.5281/zenodo.16946750, 2019.

Bikše, J., Retike, I., Haaf, E., and Kalvāns, A.: Assessing automated gap imputation of regional scale groundwater level data sets with typical gap patterns, Journal of Hydrology, 620, 129 424, https://doi.org/https://doi.org/10.1016/j.jhydrol.2023.129424, 2023.

Bloomfield, J. P. and Marchant, B. P.: Analysis of groundwater drought building on the standardised precipitation index approach, Hydrology and Earth System Sciences, 17, 4769–4787, https://doi.org/10.5194/hess-17-4769-2013, 2013.

Bloomfield, J. P., Marchant, B. P., Bricker, S. H., and Morgan, R. B.: Regional analysis of groundwater droughts using hydrograph classification, Hydrology and Earth System Sciences, 19, 4327–4344, https://doi.org/10.5194/hess-19-4327-2015, 2015.

Bloomfield, J. P., Marchant, B. P., and McKenzie, A. A.: Changes in groundwater drought associated with anthropogenic warming, Hydrology and Earth System Sciences, 23, 1393–1408, https://doi.org/10.5194/hess-23-1393-2019, 2019.

Chávez García Silva, R., Reinecke, R., Copty, N. K., Barry, D. A., Heggy, E., Labat, D., Roggero, P. P., Borchardt, D., Rode, M., Gómez-Hernández, J. J., Jomaa, S., et al.: Multi-decadal groundwater observations reveal surprisingly stable levels in southwestern Europe, Communications Earth & Environment, 5, 387, https://doi.org/10.1038/s43247-024-01554-w, 2024.

CLMS and EEA: CORINE Land Cover (CLC) 2018, Version 2020_20u1, https://land.copernicus.eu/en/products/corine-land-cover/clc2018, copernicus Land Monitoring Service, coordinated by the European Environment Agency, 2020.

Collenteur, R. and Moeck, C.: The Swiss Groundwater Database, https://doi.org/10.5281/zenodo.14260400, 2026.

Collenteur, R. A., Bakker, M., Caljé, R., Klop, S. A., and Schaars, F.: Pastas: Open Source Software for the Analysis of Groundwater Time Series, Groundwater, 57, 877–885, https://doi.org/10.1111/gwat.12925, 2019.

DHI GRAS: Report on EU-DEM Statistical Validation, Final report Specific Contract No. 3436/B2014/R0-GIO/EEA.55694, European Environment Agency, https://ec.europa.eu/eurostat/documents/7116161/7172326/Report-EU-DEM-statistical-validation-August2014.pdf, prepared for the European Environment Agency, 2014.

do Nascimento, T. V. M. et al.: EStreams: An integrated dataset and catalogue of streamflow, hydro-climatic and landscape variables for Europe, Scientific Data, 11, 879, https://doi.org/10.1038/s41597-024-03706-1, 2024.

DOV: Databank Ondergrond Vlaanderen: Grondwater, https://www.dov.vlaanderen.be, last access: 20 August 2026, 2026.

EEA: European Catchments and Rivers Network System (ECRINS), version 1, https://www.eea.europa.eu/data-and-maps/data/european-catchments-and-rivers-network, published 13 June 2012, 2012.

https://doi.org/10.5194/essd-2026-748
Preprint. Discussion started: 5 November 2026
© Author(s) 2026. CC BY 4.0 License.



EEA: Europe's state of water 2024: the need for improved water resilience, Tech. Rep. 07/2024, European Environment Agency, https://doi.org/10.2800/02236, 2024.

EEA: Waterbase WISE State of Environment (SoE), https://www.eea.europa.eu/en/datahub/datahubitem-view/208518d1-ffe3-4981-9cae-13264cd9c32c, published 12 Jul 2024; last modified 12 Mar 2026, 2026.

EuroGeoSurveys: European Geological Data Infrastructure, https://www.europe-geology.eu/, homepage; accessed 8 April 2026, 2026.

Eurostat: GISCO Countries 2024, administrative boundaries at 1:1 million scale, https://ec.europa.eu/eurostat/web/gisco/geodata/administrative-units/countries, © EuroGeographics for the administrative boundaries; last access: 26 October 2026, 2024.

Geological Service for Europe: Geological Service for Europe, https://www.geologicalservice.eu/, accessed 27 May 2026, 2026.

Gomez, M., Aguilera, H., Koch, J., Zaadnoordijk, W. J., Arnó, G., Colomer, M., Marchant, B., Brauns, B., van der Keur, P., Hinsby, K., and Broda, S.: EUGM_preprocessing, https://github.com/mgomezo12/EUGM_preprocessing, 2026a.

Gomez, M., Aguilera, H., Koch, J., Zaadnoordijk, W. J., Arnó, G., Colomer, M., Marchant, B., Brauns, B., van der Keur, P., Hinsby, K., and Broda, S.: Analysis-ready European Groundwater Monitoring (EUGM) database, https://doi.org/10.5281/zenodo.21891416, 2026b.

Hellwig, J., de Graaf, I. E. M., Weiler, M., and Stahl, K.: Large-Scale Assessment of Delayed Groundwater Responses to Drought, Water Resources Research, 56, e2019WR025 441, https://doi.org/10.1029/2019WR025441, 2020.

Hersbach, H., Bell, B., Berrisford, P., Hirahara, S., Horányi, A., Muñoz-Sabater, J., Nicolas, J., Peubey, C., Radu, R., Schepers, D., Simmons, A., Soci, C., Abdalla, S., Abellan, X., Balsamo, G., Bechtold, P., Biavati, G., Bidlot, J., Bonavita, M., De Chiara, G., Dahlgren, P., Dee, D., Diamantakis, M., Dragani, R., Flemming, J., Forbes, R., Fuentes, M., Geer, A., Haimberger, L., Healy, S., Hogan, R. J., Hólm, E., Janisková, M., Keeley, S., Laloyaux, P., Lopez, P., Radnoti, G., de Rosnay, P., Rozum, I., Vamborg, F., Villaume, S., and Thépaut, J.-N.: The ERA5 global reanalysis, Quarterly Journal of the Royal Meteorological Society, 146, 1999–2049, https://doi.org/10.1002/qj.3803, 2020.

IGRAC: Global Groundwater Monitoring Network (GGMN), https://ggis.un-igrac.org/view/ggmn/, accessed 13 April 2026, 2026.

IOOS: Manual for Real-Time Quality Control of Water Level Data: A Guide to Quality Control and Quality Assurance for Water Level Observations, Version 2.0, Tech. rep., U.S. Department of Commerce, NOAA, https://doi.org/10.25607/OBP-1466, .U.S. Integrated Ocean Observing System, 2016.

Klingler, C., Schulz, K., and Herrnegger, M.: LamaH-CE: LArge-SaMple DAta for Hydrology and Environmental Sciences for Central Europe, Earth System Science Data, 13, 4529–4565, https://doi.org/10.5194/essd-13-4529-2021, 2021.

Kumar, M. N., Murthy, C. S., Sesha Sai, M. V. R., and Roy, P. S.: On the use of Standardized Precipitation Index (SPI) for drought intensity assessment, Meteorological Applications, 16, 381–389, https://doi.org/10.1002/met.136, 2009.

Marchant, B. P., Cuba, D., Brauns, B., and Bloomfield, J. P.: Temporal interpolation of groundwater level hydrographs for regional drought analysis using mixed models, Hydrogeology Journal, 30, 1801–1817, https://doi.org/10.1007/s10040-022-02528-y, 2022.

Muñoz-Sabater, J., Dutra, E., Agustí-Panareda, A., Albergel, C., Arduini, G., Balsamo, G., Boussetta, S., Choulga, M., Harrigan, S., Hersbach, H., Martens, B., Miralles, D. G., Piles, M., Rodríguez-Fernández, N. J., Zsoter, E., Buontempo, C., and Thépaut, J.-N.: ERA5-Land: a state-of-the-art global reanalysis dataset for land applications, Earth System Science Data, 13, 4349–4383, https://doi.org/10.5194/essd-13-4349-2021, 2021.

Naz, B. S., Sharples, W., Ma, Y., Goergen, K., and Kollet, S.: Continental-scale evaluation of a fully distributed coupled land surface and groundwater model, ParFlow-CLM (v3.6.0), over Europe, Geoscientific Model Development, 16, 1617–1639, https://doi.org/10.5194/gmd-16-1617-2023, 2023.

https://doi.org/10.5194/essd-2026-748
Preprint. Discussion started: 5 November 2026
© Author(s) 2026. CC BY 4.0 License.



Nölscher, M., Mutz, M., and Broda, S.: Multiorder hydrologic Position for Europe – a Set of Features for Machine Learning and Analysis in Hydrology, Scientific Data, 9, 662, https://doi.org/10.1038/s41597-022-01787-4, 2022.

Ohmer, M., Liesch, T., Habbel, B., Heudorfer, B., Gomez, M., Clos, P., Nölscher, M., and Broda, S.: GEMS-GER: a machine learning benchmark dataset of long-term groundwater levels in Germany with meteorological forcings and site-specific environmental features, Earth System Science Data, 18, 77–95, https://doi.org/10.5194/essd-18-77-2026, 2026.

Pesaresi, M., Schiavina, M., Politis, P., Freire, S., Krasnodębska, K., Uhl, J. H., Carioli, A., Corbane, C., Dijkstra, L., Florio, P., Friedrich, H. K., Gao, J., Leyk, S., Lu, L., Maffenini, L., Mari-Rivero, I., Melchiorri, M., Syrris, V., Van Den Hoek, J., and Kemper, T.: Advances on the Global Human Settlement Layer by joint assessment of Earth Observation and population survey data, International Journal of Digital Earth, 17, 2390 454, https://doi.org/10.1080/17538947.2024.2390454, 2024.

Poggio, L., de Sousa, L. M., Batjes, N. H., Heuvelink, G. B. M., Kempen, B., Ribeiro, E., and Rossiter, D.: SoilGrids 2.0: producing soil information for the globe with quantified spatial uncertainty, SOIL, 7, 217–240, https://doi.org/10.5194/soil-7-217-2021, 2021.

TNO-GDN: Groundwater head viewer, https://www.grondwatertools.nl/gwsinbeeld, accessed: 31 July 2026, 2024.

Winckel, A., Ollagnier, S., and Gabillard, S.: Managing groundwater resources using a national reference database: the French ADES concept, SN Applied Sciences, 4, 217, https://doi.org/10.1007/s42452-022-05082-0, 2022.

Zaadnoordijk, W. J. and Lourens, A.: Groundwater Dynamics in the Aquifers of the Netherlands, Tech. Rep. TNO 2019 R12031, TNO Geological Survey of the Netherlands, Utrecht, The Netherlands, https://www.grondwatertools.nl/sites/default/files/2023-07/ZaadnoordijkLourens2019_GroundwaterDynamicsInTheAquifersOfTheNetherlands_TNO-R12031.pdf, 2019.